

## Instrumentation System for Thermal Analysis of Electro-Explosive Devices

D. K. Kankane, S. N. Ranade, R. B. Sohoni and G. S. Deshpande  
*High Energy Materials Research Laboratory, Pune - 411 021.*

### ABSTRACT

A constant current pulser, with adjustable pulse width and current, is designed to evaluate thermal characteristics of electro-explosive devices (EED). The thermal response in voltage/time profile is digitised and recorded on a PC. A software for the analysis of this data has been developed. It computes the heat loss coefficient ( $\gamma$ ), thermal capacity ( $C_{\theta}$ ) and thermal time constant ( $\tau$ ) of the system. These parameters are used for the prediction of the performance EEDs during development stage and also in quality control. A computerised system developed for this purpose is also described in detail.

### 1. INTRODUCTION

In an electro-explosive device (EED), its firing current causes the bridge wire to heat up to the ignition temperature of the composition surrounding it. To assess the characteristics of EEDs, non-destructive test (NDT) is carried out. In this test, a constant current, less than its firing current, is passed through the bridge wire. This heats up the bridge wire causing change in its resistance which is measured as voltage drop across the bridge wire. The EED under test is a part of Whetstone bridge which is initially balanced, so the imbalance recorded is only due to change in resistance. This imbalance profile recorded in the voltage/time form is analysed to determine the temperature rise  $\theta_{max}$ , heat loss coefficient ( $\gamma$ ), thermal capacity ( $C_{\theta}$ ) and thermal time constant ( $\tau$ ) of the EED<sup>1</sup>.

Prior to the development of this system, the EEDs were destructively tested for their ignition

delay and firing current, using oscilloscopes and countertimers. The NDT facility using a current source and oscilloscope was used. However, the measurements of graphs and calculations involved in thermal analysis were too complex for routine testing. With this system, it is very easy to test all the EEDs under development or production.

### 2. CIRCUIT DESCRIPTION

The block schematic of the system is given in Fig. 1. The system designed is mainly in two parts – a constant current source and a signal amplification unit (Fig. 2) and one PC-compatible circuit board for digitisation of the signal (Fig. 3). The constant current source is designed using a voltage regulator integrated circuit (U3). The voltage regulator integrated circuit maintains constant voltage across a high stability potentiometer (P1) resulting in a constant current of amplitude as per the setting of the potentiometer. This current source is designed

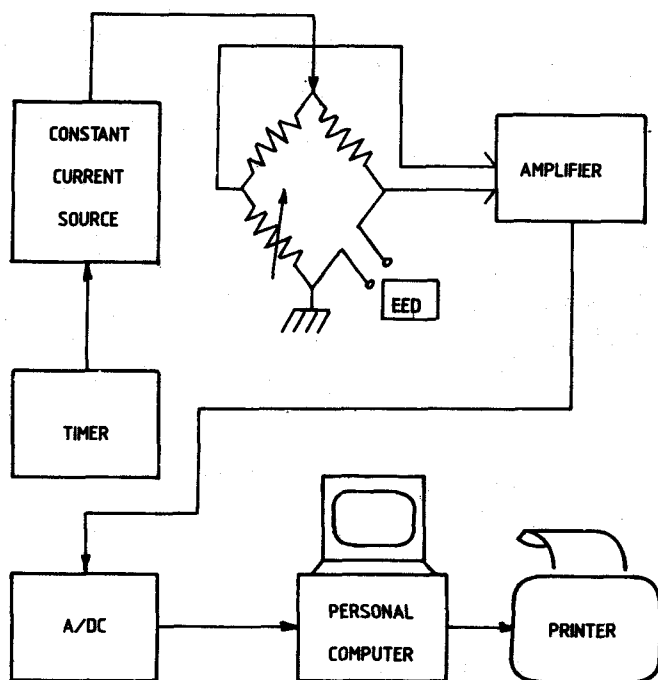


Figure 1. Block schematic of the system

to deliver current up to 500 mA. During the current setup procedure, the current is passed through a high precision resistance of  $1\Omega$  (R15) and the voltage across it is measured and displayed on a digital panel meter. A timer circuit (U1) controls the duration of the test current pulse which can be set from 10 to 500 ms with the help of a calibrated dial potentiometer (P2) on the front panel of the unit. The unit can test EEDs having resistance up to  $12\Omega$ . The test current is applied to the Whetstone bridge circuit in which the EED is connected as one arm of the bridge. Initially, the bridge is balanced by passing the test current for a very short duration of 5 ms and adjusting a potentiometer (P3). During test, the bridge imbalances due to heating of EED's bridge wire. This imbalance is of the order of fraction of a millivolt due to very small change in resistance ( $\delta R$ ) of the EED values. An instrumentation amplifier circuit (U4-U7) amplifies and converts this differential signal into a single ended, low-output impedance signal of about 1V amplitude. This signal is acquired by the PC-compatible digitiser board designed for this

purpose. A trigger signal derived from the current pulse timing circuit is also provided for synchronisation. The digitiser circuit uses an 8-bit A/D circuit (U12) for data acquisition. A crystal-controlled clock (U25, U24) and a programmable timer/counter (U10) is used for accurate and software-programmed sample rate generation. The A/D circuit outputs are connected to the PC bus through a programmable parallel port (U11). The acquisition is done through software control. A software programmable gain amplifier (U16, U17, U20, U21) is designed to facilitate signal acquisition with programmable range selection.

Initially, the EED under test is connected to the unit. The test current is set to the required level with the help of the digital panel meter. The bridge is balanced by zeroing the imbalance trace on the computer screen, caused by a 5 ms pulse of the test current. During the test, current is applied for a duration of about 200 to 500 ms and 500 samples are acquired. The data is displayed on the computer screen as voltage/time graph. The operator indicates the stable temperature ( $\theta_{max}$ ) with the help of a cursor on the screen. Slope is determined by applying straight line least square fit (LSF) to the rising portion of the voltage-time profile. A typical graph along with the computed thermal parameters of the EED under test is shown in Fig. 4. The software for the system is developed in Turbo C. The data acquisition and digitiser setup routines are written in Assembly language and linked to the system software

### 3. THEORY OF OPERATION

Considering EED as one system consisting of explosives in the vicinity of bridge wire and neglecting the temperature rise due to chemical reaction, energy equation<sup>1</sup> is given by

$$I^2 R_o (1 + \alpha\theta) dt = C_o d\theta + \gamma\theta dt \quad (1)$$

where

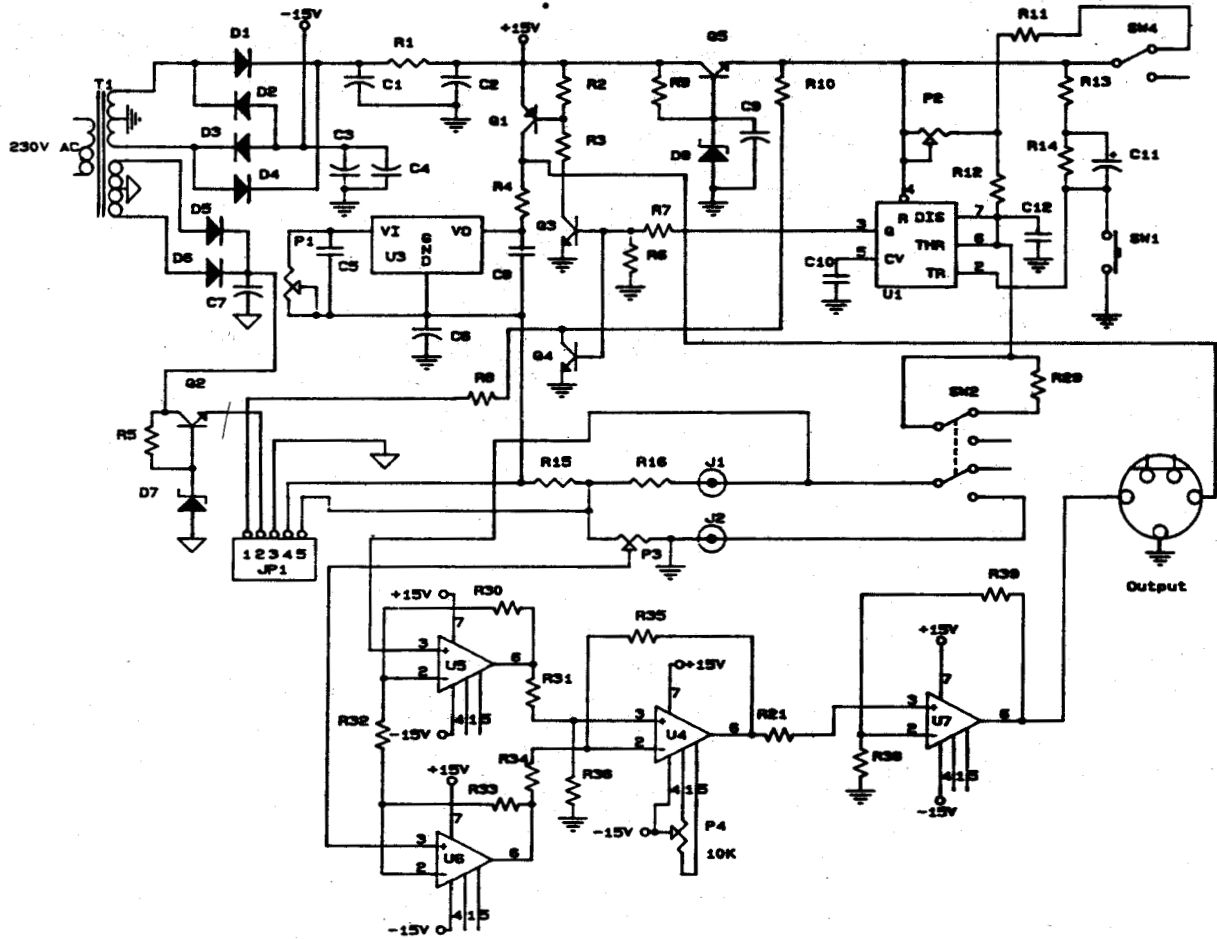


Figure 2. Constant current source and a signal amplification unit

- $I$  = Test current
- $R_o$  = Resistance of the EED bridge wire
- $\alpha$  = Temp. coefficient of bridge wire material
- $\theta$  = Temperature rise above ambient
- $C_\theta$  = Thermal capacity of the system
- $\gamma$  = Heat loss coefficient for the system.

The solution for  $\theta$  in terms of  $I$  with  $C_\theta$  and  $\gamma$  as unknowns works out as

$$\theta = \frac{I^2 R_o}{\gamma - \alpha I^2 R_o} \left( 1 - \exp - \frac{(\gamma - \alpha I^2 R_o)t}{C_\theta} \right) \quad (2)$$

As  $t \rightarrow \infty$

$$\theta_{max} = \frac{I^2 R_o}{\gamma - \alpha I^2 R_o} \quad (2a)$$

The voltage developed across bridge wire ( $R_o$ ) due to current  $I$  is given by

$$V = IR_o (1 + \alpha\theta) \quad (3)$$

This expression also gives

$$\theta_{max} = \frac{V_{max}}{\alpha IR_o} \quad (3a)$$

Substituting the expression for  $\theta$  as per Eqn (2) above in Eqn (3) one gets:

$$V = IR_o + \frac{\alpha I^3 R_o^2}{\gamma - \alpha I^2 R_o} \left( 1 - \exp \left( - \frac{(\gamma - \alpha I^2 R_o)t}{C_\theta} \right) \right)$$

The first term,  $IR_o$  is zero as the bridge is balanced, initially. The bridge unbalance, i.e., the

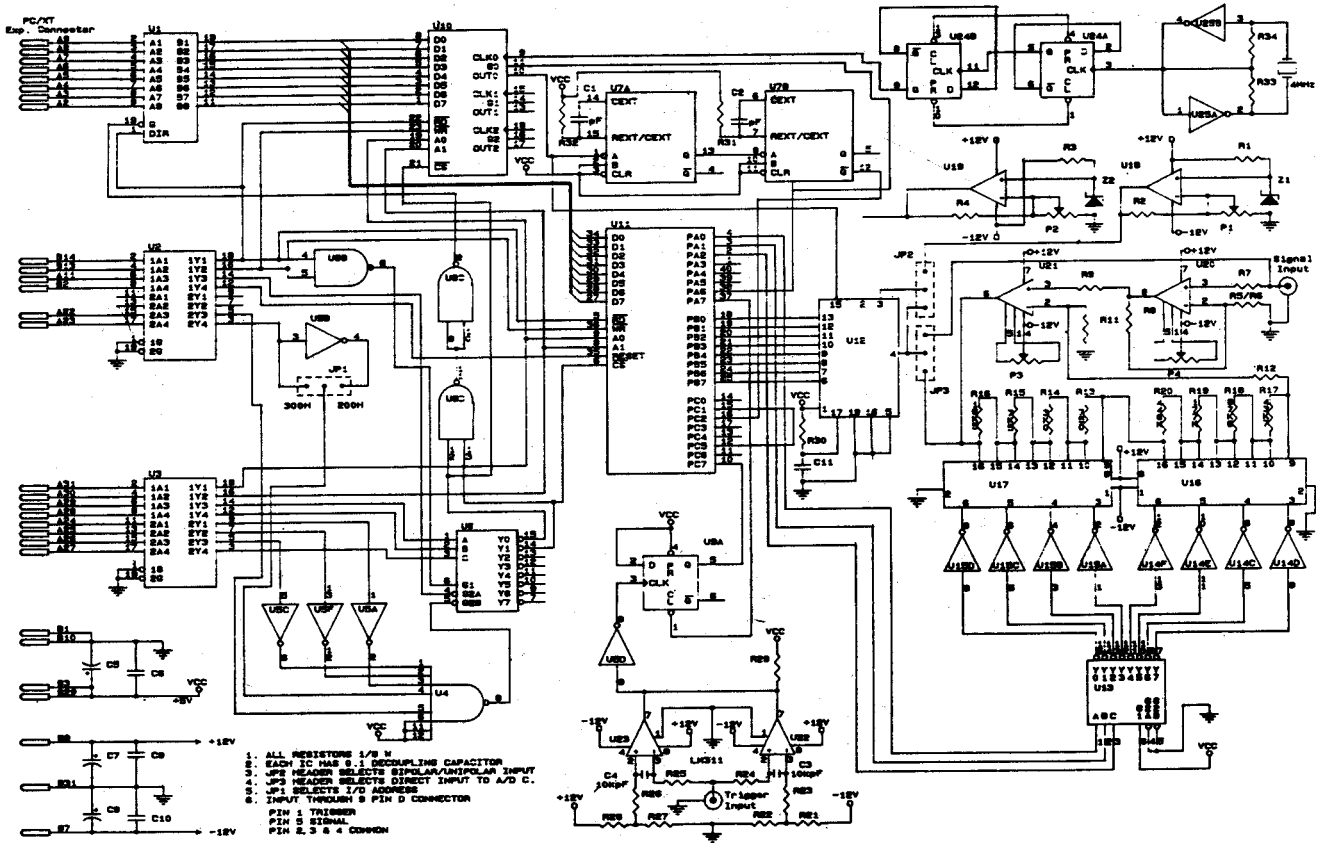


Figure 3. PC-compatible circuit board for digitisation of the signal

voltage developed only due to temperature rise is measured and would be

$$\Delta V = \frac{\alpha I^3 R_o^2}{\gamma - \alpha I^2 R_o} \left( 1 - \exp\left(-\frac{(\gamma - \alpha I^2 R_o)t}{C_0}\right) \right) \quad (4)$$

This voltage is digitised and recorded. With this voltage-time profile, constants like  $C_0$ ,  $\gamma$  and  $\tau$  can be computed.

The Eqn (4) is of the exponential form

$$\Delta V = V_{max} \left( 1 - \exp\left(\frac{-t}{\tau}\right) \right) \quad (5)$$

where

$$V_{max} = \frac{\alpha I^3 R_o^2}{\gamma - \alpha I^2 R_o} \quad (6)$$

and

$$\tau = \frac{C_0}{\gamma - \alpha I^2 R_o} \quad (7)$$

where  $\tau$  is thermal-time constant and can be determined from the voltage-time profile as explained here.

$C_0$  and  $\gamma$  can be computed from Eqns (6) and (7) as given

$$C_0 = \frac{\alpha I^3 R_o^2 \tau}{V_{max}} \quad \text{and} \quad \gamma = \frac{\alpha I^3 R_o^2}{V_{max}} + \alpha I^2 R_o$$

Thermal-time constant  $\tau$  is computed by finding the time ( $t_{1/2}$ ), up to  $V_{max}/2$  from  $t = 0$ . Then

$$\tau = \frac{t_{1/2}}{\ln 2}$$

Alternately,  $C_0$  can be computed by differentiating Eqn(4) wrt time. This leads to

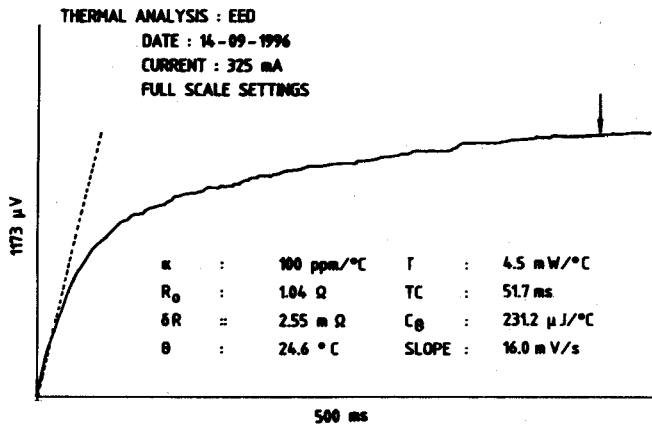


Figure 4. Voltage-time graph and computed parameters of a typical EED.

$$C_\theta = \frac{\alpha I^3 R_0^2}{S}$$

where  $S$  is the slope at  $t = 0$ . Slope is determined by applying straight line LSF to the rising portion of the voltage-time profile. The curve fitting is applied to the data points up to  $V_{max}/4$  level. From the slope  $\tau$  can also be calculated as

$$\tau = \frac{V_{max}}{S}$$

where  $C_\theta$  and  $r$  are constants for the EED, and the maximum temperature rise due to the current can be determined using these.

#### 4. EXPERIMENT

Different types of EEDs of known ‘no-fire’ and ‘all-fire’ currents were tested for thermal analysis at below ‘no-fire’ currents. Tables 1 and 2 show the results of two types, calculated for each of the EEDs when subjected to different test currents. The tables show two columns each for  $C_\theta$ ,  $\tau$  and  $\theta_{max}$ .  $C_\theta$  and  $\tau$  are computed by both the methods (slope and  $t_{1/2}$ ) described above. The last column shows computed temperatures determined from Eqn (2a) using  $\gamma$  values determined experimentally. The  $\theta_{max}$  at any safe current can be predicted by Eqn (2a) and to show the accuracy of prediction, the  $\theta_{max}$  values calculated at the same currents are tabulated in Tables 1 and 2.

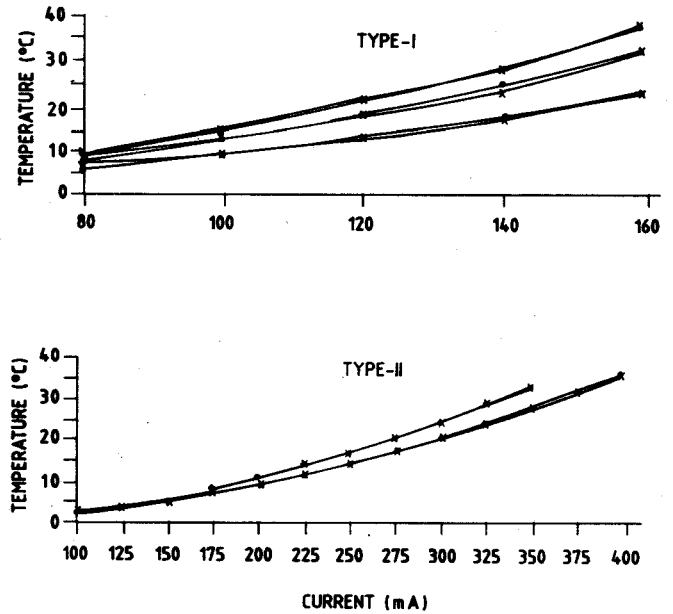


Figure 5. Temperature vs current graphs of type-I and type-II EEDs.

Five EEDs of type-I were tested for five different test currents from 80 to 160 mA at five different occasions. Thermal parameters  $\theta_{max}$ ,  $\gamma$ ,  $C_\theta$  and  $\tau$  were averaged for a specific test current and are shown in Table 1. Four EEDs of type-II were tested for 8 to 13 different test currents for one occasion and the parameters are shown in Table 2. A typical graph of imbalance voltage-time profile is shown in Fig. 4. The straight line at the start of the graph is the LSF line. Figure 5 shows graphs of calculated and measured  $\theta_{max}$  values vs test current.

#### 5. CONCLUSION

- The instrumentation system developed for NDT of EED is working satisfactorily and is very useful for the thermal analysis of EEDs. This system tests EEDs up to 500 mA of test currents and for 500 ms test duration. A separate current Pulser unit for higher test currents can be developed if required. The software developed will be useful for analysis at higher currents also.
- From the tables it is observed that there is a good correlation between experimentally measured and theoretically calculated temperatures at the respective currents. The

Table 1. Test results of type-1 EEDs

No./R <sub>0</sub> (Ω)	Current (mA)	θ <sub>max</sub> (°C)	γ (mW/°C)	C <sub>θ</sub>		τ (ms)	t		θ <sub>c</sub> (°C)
				(μJ/°C)	LSF method		(μJ/°C)	t <sub>1/2</sub> method	
IC/1.86	80	9.6	1.268	46.832		36.270	38.940	30.470	9.5
IC/1.86	100	14.5	1.294	42.508		32.846	40.436	31.162	14.8
IC/1.86	120	22.1	1.222	35.934		29.404	34.476	28.218	21.4
IC/1.86	140	28.6	1.285	38.664		30.132	35.690	27.874	29.1
IC/1.86	160	38.8	1.238	41.412		33.552	37.822	30.644	38.1
Averages			1.261	41.070		32.441	37.473	29.674	
2C/2.26	80	7.5	2.088	54.360		23.114	55.930	24.236	5.8
2C/2.26	100	9.1	2.523	71.560		27.732	57.600	22.678	9.0
2C/2.26	120	12.3	2.645	65.700		24.812	61.366	23.198	13.0
2C/2.26	140	16.7	2.665	65.110		24.470	62.280	23.370	17.7
2C/2.26	160	22.6	2.578	62.388		24.276	59.784	23.198	23.2
Averages			2.500	63.824		24.881	59.392	23.336	
3C/1.86	80	8.9	1.353	33.000		24.054	29.484	21.812	8.1
3C/1.86	100	12.9	1.447	40.622		28.184	33.768	23.370	12.7
3C/1.86	120	17.9	1.508	39.124		25.900	32.660	21.642	18.3
3C/1.86	140	23.5	1.560	33.496		21.550	33.122	21.294	24.9
3C/1.86	160	32.5	1.471	40.006		27.232	33.474	22.854	32.5
Averages			1.468	37.250		25.384	32.502	22.194	
4C/1.86	80	10.3	1.170	30.304		25.504	25.170	21.466	8.9
4C/1.86	100	13.6	1.369	30.542		22.406	29.562	21.642	14.0
4C/1.86	120	19.5	1.377	31.784		23.084	29.578	21.466	20.1
4C/1.86	140	26.1	1.402	29.948		21.442	29.266	20.946	27.4
4C/1.86	160	35.4	1.352	30.450		22.610	29.142	21.642	35.8
Averages			1.334	30.606		23.009	28.544	21.432	
5C/2.04	80	7.8	1.703	41.432		24.338	41.176	23.892	7.2
5C/2.04	100	11.6	1.766	56.376		31.854	45.828	25.968	11.3
5C/2.04	120	15.7	1.883	52.134		27.748	48.546	25.796	16.2
5C/2.04	140	21.4	1.875	46.132		24.644	42.092	22.508	22.1
5C/2.04	160	28.6	1.831	53.914		29.554	48.040	26.312	28.9
Averages			1.812	49.998		27.628	45.136	24.895	

temperature vs current graphs are showing good agreement between measured and computed values.

- From this analysis, it is seen that temperatures at other higher currents below safe current can be calculated to a reasonable degree of accuracy.
- From the experiments, it is observed that there is considerable variation in C<sub>θ</sub> and τ values computed by slope method compared to those computed by t<sub>1/2</sub> method. This may

be due to limited availability of data points for determination of slope by LSF method.

- The temperature-time curve being exponential, the thermal-time constant τ may lead to determination of the ignition delay.
- The temperatures given by this method are average temperatures of the EED across the bridge wire. Actual temperature rise at the centre of the bridge wire is likely to be at a higher level, as reported. This is due to the

Table 2. Test results of type-II EEDs

No./R <sub>0</sub> ( $\Omega$ )	Current (mA)	$\theta_{max}$ ( $^{\circ}\text{C}$ )	$\gamma$ (mW/ $^{\circ}\text{C}$ )	$C_{\theta}$		$\tau$ (ms)	$C_{\theta}$		$\tau$ (ms)	$\theta_c$ ( $^{\circ}\text{C}$ )
				( $\mu\text{J}/^{\circ}\text{C}$ )	(ms)		( $\mu\text{J}/^{\circ}\text{C}$ )	(ms)		
				LSF method		$t_{1/2}$ method				
ID/1.04	100	2.89	3.60	115.38	32.09	129.67	36.07	2.34		
ID/1.04	125	3.92	4.14	183.59	44.33	191.19	46.17	3.66		
ID/1.04	150	4.48	5.23	273.53	52.38	293.83	56.27	5.27		
ID/1.04	175	7.61	4.18	180.15	43.10	198.99	47.61	7.17		
ID/1.04	200	9.32	4.46	232.98	52.26	212.26	47.61	9.37		
ID/1.04	225	11.62	4.53	241.04	53.25	248.17	54.82	11.86		
ID/1.04	250	14.99	4.34	184.13	42.50	193.76	44.72	14.65		
ID/1.04	275	16.99	4.63	241.10	52.14	233.49	50.49	17.73		
ID/1.04	300	20.57	4.56	226.65	49.86	229.52	50.49	21.11		
ID/1.04	325	24.55	4.48	231.16	51.71	225.71	50.49	24.79		
ID/1.04	350	28.21	4.52	242.88	53.84	240.81	53.38	28.76		
ID/1.04	375	32.49	4.51	225.23	50.09	233.54	51.94	33.03		
ID/1.04	400	36.51	4.57	235.71	51.76	243.07	53.38	37.59		
Averages			4.44	216.43	48.41	221.08	49.50			
2D/1.00	175	8.52	3.596	144.42	40.20	118.17	32.89	8.54		
2D/1.00	200	11.36	3.527	102.18	29.01	112.82	32.03	11.16		
2D/1.00	225	14.45	3.508	112.68	32.17	106.12	30.30	14.13		
2D/1.00	250	17.22	3.635	116.41	32.08	122.51	33.76	17.45		
2D/1.00	300	24.80	3.637	138.05	38.05	131.91	36.36	25.15		
2D/1.00	325	29.74	3.563	121.54	34.22	122.99	34.62	29.53		
2D/1.00	350	33.69	3.649	133.09	36.60	135.36	37.22	34.26		
Averages			3.588	124.05	34.62	121.41	33.88			
3D/1.04	175	6.27	5.076	188.97	37.26	219.53	43.28	6.74		
3D/1.04	200	7.46	5.575	265.09	47.59	274.85	49.34	8.80		
3D/1.04	225	13.91	3.788	104.72	27.68	98.23	25.97	11.15		
3D/1.04	250	14.81	4.391	128.48	29.31	151.80	34.62	13.76		
3D/1.04	275	16.67	4.721	187.78	39.84	187.67	39.82	16.66		
3D/1.04	300	20.77	4.511	149.03	33.11	136.38	30.30	19.83		
3D/1.04	325	23.18	4.745	191.49	40.45	151.62	32.03	23.28		
3D/1.04	350	25.78	4.950	174.91	35.43	162.41	32.89	27.01		
3D/1.04	375	30.51	4.804	176.72	36.90	182.40	38.09	31.02		
Averages			4.729	174.13	36.40	173.88	36.26			
4D/1.01	200	7.86	5.137	154.14	30.03	119.97	23.37	7.55		
4D/1.01	225	9.13	5.594	170.22	30.46	154.82	27.70	9.56		
4D/1.01	250	13.44	4.700	100.83	21.48	101.56	21.64	11.81		
4D/1.01	275	15.86	4.813	125.30	26.07	120.64	25.10	14.29		
4D/1.01	325	17.99	5.927	184.17	31.13	143.40	24.24	19.97		
4D/1.01	350	22.46	5.510	135.23	24.60	147.51	26.83	23.17		
4D/1.01	375	24.54	5.790	166.33	28.80	164.98	28.57	26.60		
Averages			5.353	148.03	27.51	136.13	25.35			

heat sink effect of the connection wires of the bridge and the composition. Determination of the highest temperature along the bridge wire for a specific current may be attempted with the parameters made available by this test.

#### ACKNOWLEDGEMENTS

The authors are grateful to Dr Haridwar Singh, Director, HEMRL, Pune, for granting permission to publish this paper. The authors are thankful to

Sarvashri S. Jayaraman, N. L Varyani, B.G. Khair, and S. M. Deshmukh of HEMRL Pune, for their continuous cooperation and suggestions.

#### REFERENCES

1. Rosenthal, L.A. & Menichelli, V. J. Non-destructive testing of insensitive electro-explosive devices by transient techniques. Jet Propulsion Laboratory, Pasadena, California, 15 July, 1970. TR-JPL- 32-1494.

#### Contributors



**Mr DK Kankane** obtained his MSc (Physics) from University of Poona and MTech (Transducer Physics and Instrumentation) from IIT, Madras. He joined DRDO at the High Energy Materials Research Laboratory, Pune, in 1983. Presently, he is working as Scientist E. His areas of research include design and development of controllers and instrumentation systems for assessment of high energy materials and software development for the systems.



**Mr SN Ranade** obtained his diploma in Electronics and Communication Engineering (DECE). He joined DRDO at the HEMRL, Pune, in 1972. Presently, he is working as Technical Officer B. His areas of research include design and development of controllers and instrumentation systems for assessment of high energy materials and software development for the systems.



**Mr RB Sohoni** obtained his diploma in Electronics and Communication Engineering (DECE). He joined DRDO at the HEMRL, Pune, in 1972. Presently, he is working as Technical Officer B. His areas of research include design and development of controllers and instrumentation systems for assessment of high energy materials and software development for the systems.